ACS OMEGA

Article

Cite This: ACS Omega 2019, 4, 3322−3328

http://pubs.acs.org/journal/acsodf

Dual Stimuli-Responsive Block Copolymers for Controlled Release Triggered by Upconversion Luminescence or Temperature Variation

Yueh-Chi Chung,[†] Chien-Hsin Yang,[†] Rong-Ho Lee,[‡] and Tzong-Liu Wang*[,†]

[†]Department of Chemical and Materials Engineering, National University of Kaohsiung, Kaohsiung 811, Taiwan, Republic of China

[‡]Department of Chemical Engineering, National Chung Hsing University, Taichung 402, Taiwan, Republic of China

Supporting Information

ABSTRACT: An amphiphilic block copolymer (BCP) which contains both photoresponsive and thermoresponsive blocks was synthesized by the atom transfer radical polymerization approach. Meanwhile, a new core/shell type of the upconversion nanoparticle (UCNP) $LiYF_4:Yb^{3+}_{0.25},Tm^{3+}_{0.01}@LiYF_4:Yb^{3+}_{0.2}$ was successfully synthesized. By encapsulating UCNPs inside the micelles of the BCP and incorporating Nile red (NR) into the UCNP@BCP hybrid nanoparticles as a model drug, controlled release of the drug by the dual-stimuli BCP could be studied. After exposing the UCNP-loaded micellar solution to near-infrared (NIR) light, it was found that the UV light pumped from UCNPs could disrupt the polymer micelles and the fluorescence intensity of NR decreased with the increase of the irradiation time of the NIR light. The thermoresponsive study indicated that the fluorescence intensity of NR decreased with the increase of temperature of the micellar solution because of the release of NR into water arising from the contraction of the amphiphilic BCP.

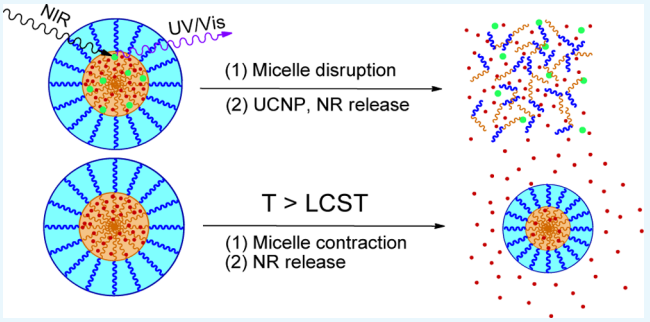

1. INTRODUCTION

In recent years, stimuli-sensitive materials have attracted considerable attention in a vast variety of applications. Among them, stimuli-responsive polymers have gained practical and enhanced interests owing to their response to external stimuli such as variation of temperature, light, pH, pressure, magnetic and electric fields, and so forth.[1−6] Multistimuli-responsive polymers have recently been paid more attention because of the variation in property control.[7−10] To trigger the multistimuli action, the stimuli-responsive polymer must possess a block copolymer (BCP) structure with each block facilitating the response to the variation of environmental conditions such as temperature, light, and so forth. In addition, the BCP is often a type of amphiphilic micelle in aqueous media for biomedical applications. By incorporating appropriate photoresponsive moieties into a BCP, the polymeric micelles can be disrupted through photochemical reactions such as trans−cis isomerization, molecular dimerization, and bond cleavage. Alternatively, a temperature-sensitive polymer can be transferred from a hydrophilic state to a hydrophobic state when the solution temperature is raised above the lower critical solution temperature (LCST). Hence, this type of polymer is also frequently used as a stimulus-responsive material in a wide range of applications.[11,12]

However, all explored photoreactions require strong radiation, such as UV or visible light, which may cause a serious injury to organisms. In this regard, triggering the action of a photoresponsive polymeric micelle by near-infrared (NIR) light may be an appealing alternative because of the less detrimental radiation and deeper penetration compared to ultraviolet/visible (UV/vis) light. To achieve this goal, lanthanide-doped upconversion nanoparticles (UCNPs) for use in converting NIR radiation into UV/vis light have been recently developed.[13,14] By employing this method, combining UCNPs and photoresponsive polymers in hybrid nanocapsules has become a widely applied strategy for use in NIR-triggered drug delivery.[15−19]

UCNPs are usually composed of lanthanide-doped transition metals and are dilute guest−host systems. Lanthanide ions are dispersed as a guest in a proper dielectric host lattice with a dimension of less than 100 nm. These Ln^{3+} ions are optically active centers and can exhibit sharp luminescence emissions via intra-4f or 4f−5d transitions.[20,21] Through judicious selection of lanthanide dopants including the sensitizer and activator, UCNPs can display anti-Stokes emission such as NIR to shorter NIR, visible, or UV light by upconversion mechanisms. In addition, selection of appropriate host materials is crucial for high-efficiency upconversion emissions. As for the host materials, $NaYF_4$ is one of the most studied material.[15,21−24] To the best of our knowledge, $LiYF_4$ is rarely studied to date. On the other hand, it has been indicated

Received: December 5, 2018
Accepted: February 4, 2019
Published: February 14, 2019

DOI: 10.1021/acsomega.8b03414
ACS Omega 2019, 4, 3322−3328

that the utilization of a core/shell structure can enhance the fluorescence intensity of UCNPs. There are three types of core/shell structures that have been utilized to enhance the photoluminescence (PL) intensity of UCNPs.[25,26] In this study, we adopt the active core/active shell structure, in which the host material and the sensitizer of the shell are the same as those of the core materials.[25−29] Owing to the sensitizer dopant in the shell, the active shell can not only protect the core from surface defects but also transfer absorbed NIR light from the pump source to the core UCNP. Therefore, the sensitizer-doped active shell can significantly enhance the fluorescence intensity of UCNPs.

This research aims to design and synthesize a dual-stimuli BCP in conjunction with the upconversion function of a new type of $LiYF_4$ core/shell UCNP for application in controlled release of drugs. The strategy is based on that hydrophobic UCNPs and water insoluble drugs tend to be entrapped in the hydrophobic core of polymer micelles, while the hydrophilic polymer shell stabilizes the whole nanocapsule in aqueous solution. The dual-stimuli BCP consists of a photosensitive block and a temperature-sensitive block which are hydrophobic and hydrophilic, respectively. Upon encapsulation of a model drug, Nile red (NR) dye, into the diblock copolymer, the phenomenon of controlled release of drugs can be monitored by the variation of the temperature. When the temperature is raised above the LCST of the thermoresponsive block, the amphiphilic BCP will shrink and squeeze NR out of the BCP. Alternatively, when both NR and $LiYF_4$ UCNPs are loaded into the amphiphilic BCP, the UV emission from UCNPs can cleave the photoresponsive block; thus, the hydrophobic core becomes hydrophilic. As a result, the polymeric micelles are disrupted and release the model drug (NR) into aqueous media.

Hence, by using the hybrid UCNP@BCP strategy, the controlled release of encapsulated molecules in the UCNP@BCP hybrid nanoparticles could be accomplished effectively by photostimulation for biomedical applications. On the other hand, to mimic the environmental change and enhance the function of drug delivery, incorporation of a temperature-sensitive segment into the polymeric micelles coupled with a photoresponsive segment could be a more effective approach for application in biotechnology.

In this study, we employed a single activator/sensitizer combination of Tm^{3+}/Yb^{3+} to prepare a new kind of lanthanide-doped core/shell UCNP. This kind of UCNP has the active core/active shell structure, which can enhance the fluorescence intensity of the UCNP significantly. Upon excitation with a 980 nm NIR laser diode, the UCNPs can emit fluorescence spanning from the UV to NIR region. Because this kind of UCNP can emit fluorescence in the UV region, which can disrupt the photoresponsive polymeric micelles to release the encapsulated molecules, the BCP employed in the encapsulation of the loaded UCNPs and the model drug should contain the photosensitive segment. In addition, a thermoresponsive polymeric segment with a LCST lower than the temperature of human body (37 °C) is thought to be suitable as the temperature-sensitive block along with the photoresponsive block in the synthesis of the dual-stimuli BCP. In aqueous media, this diblock copolymer could self-assemble into polymeric micelles with the photosensitive segments as the hydrophobic core and the thermosensitive segments as the hydrophilic shell. Upon UV irradiation, the photosensitive segments perform the photolysis reaction and trigger the dissociation of the polymeric micelles. At the temperature above the LCST, the polymeric micelles shrink because of a decrease of the hydrophilicity of the thermosensitive segments; hence, the encapsulated molecules are squeezed out. Furthermore, because it has been indicated that UV/vis light can cleave chemical groups (called photocleavable/photoremovable/photolabile groups) such as *o*-nitrobenzyl- and coumarin-based groups[30−32] and the UV light emitted from our synthesized UCNPs overlaps well with the absorption band of *o*-nitrobenzyl groups (around 362 nm), we designed an amphiphilic BCP composed of the hydrophobic block poly(*o*-nitrobenzyl acrylate) (PNBA) bearing the *o*-nitrobenzyl groups as the photosensitive block. On the other hand, because poly(*N*-alkyl (meth)acrylamide)s are perhaps the most heavily studied thermoresponsive polymers,[33] we designed the amphiphilic BCP containing poly(*N*,*N*-diethylacrylamide) (PDEAAm) as the hydrophilic block. The as-synthesized amphiphilic BCP is designated as PDEAAm-*b*-PNBA.

2. RESULTS AND DISCUSSION

The new nanocomposite UCNP@BCP was prepared and NR was encapsulated to simulate the process of controlled release of drugs. In this work, a core/shell-type UCNP with emission of UV light at 361 nm has been synthesized. In addition, a new type of dual stimuli-responsive BCP composed of a photosensitive and temperature-sensitive block by atom transfer radical polymerization (ATRP) has been synthesized (Figure 1). To our knowledge, this kind of $LiYF_4:Yb^{3+},Tm^{3+}$@

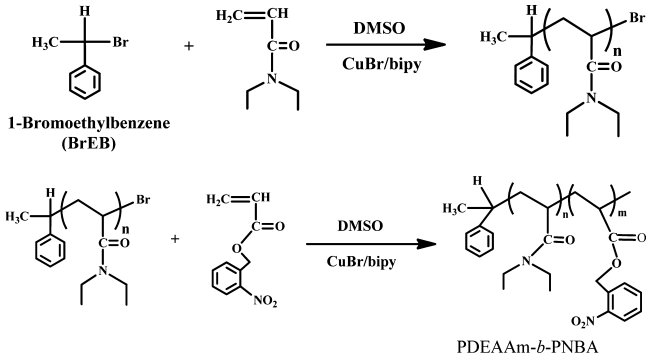

Figure 1. Synthetic route for the dual-stimuli BCP PDEAAm-*b*-PNBA via ATRP.

$LiYF_4:Yb^{3+}$ core/shell UCNP has not been studied in combination with the newly synthesized, dual stimuli-responsive BCP PDEAAm-*b*-PNBA. The controlled release triggered by the dual-stimuli approach is illustrated in Figure 2.

Wide-angle X-ray diffraction (XRD) was performed to investigate the crystal structure of the $LiYF_4:Yb^{3+}_{0.25},Tm^{3+}_{0.01}$ UCNP core and $LiYF_4:Yb^{3+}_{0.25},Tm^{3+}_{0.01}$@$LiYF_4:Yb^{3+}_{0.2}$ core/shell UCNP. From the upper XRD pattern, the sharp and intense peaks from (101), (112), and (202) planes, as shown in Figure 3, the crystal structure of the core UCNP can be indexed as the tetragonal phase (JCPDS no. 17-0874). After coating the $LiYF_4:Yb^{3+}$ shell, it shows peaks that are similar to those of the core UCNP, as evident from the lower pattern of Figure 3. Because the shell composition is almost the same as that of the core, the XRD pattern of the core/shell UCNP is very similar to the pattern of its corresponding core UCNP.

DOI: 10.1021/acsomega.8b03414
ACS Omega 2019, 4, 3322−3328

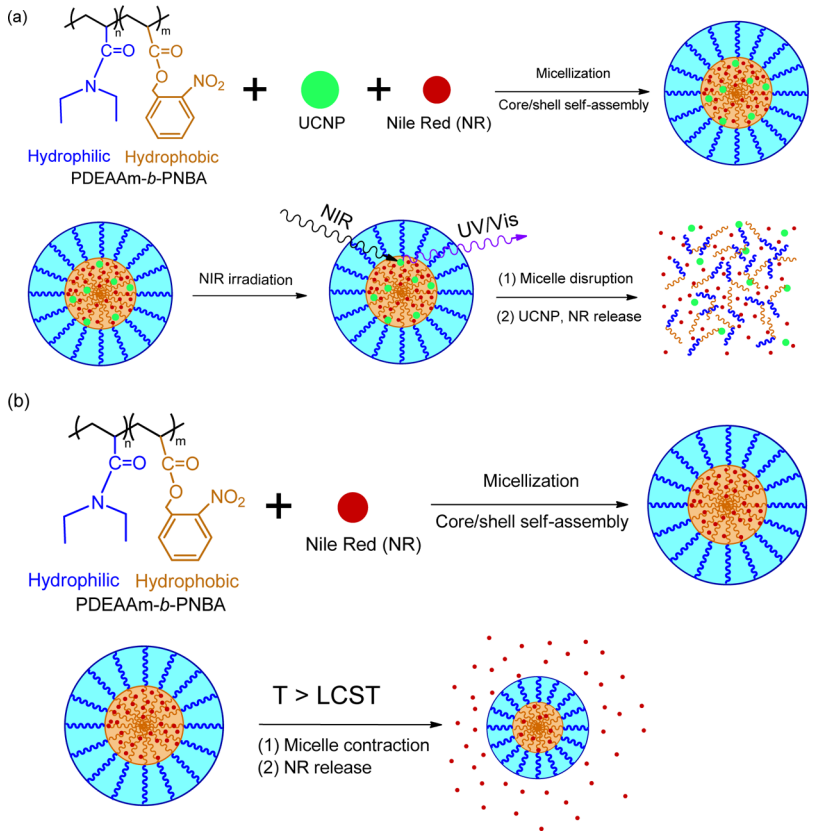

Figure 2. Schematic illustration of triggering dissociation of dual-stimuli polymeric micelles under (a) photochange or (b) temperature (UCNP unloaded)-change stimulations.

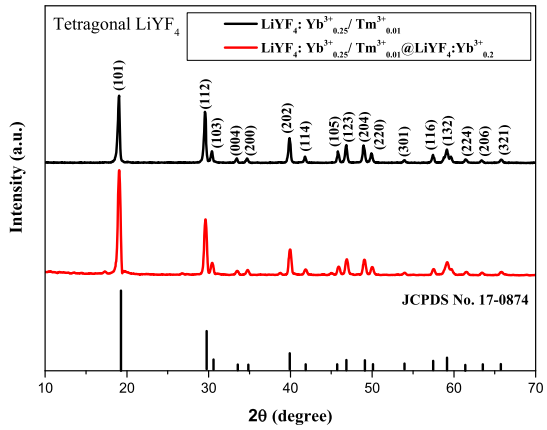

Figure 3. XRD patterns of the $LiYF_4:Yb^{3+}_{0.25},Tm^{3+}_{0.01}$ core UCNP and $LiYF_4:Yb^{3+}_{0.25},Tm^{3+}_{0.01}@LiYF_4:Yb^{3+}_{0.2}$ core/shell UCNP.

Figure 4a,b depicts the high resolution transmission electron microscopy (HRTEM) images of the core and core/shell UCNP. As seen from these images, both the core UCNP and core/shell UCNP appear to be rhombus-shaped and monodispersed under high magnification (×500 K). The aspect ratio (length/breadth) of the diagonal is ca. 1.35 for the core UCNP and 1.64 for the core/shell UCNP. After shell coverage, both diagonal lengths of the core/shell UCNP increase significantly. This confirms the formation of the $LiYF_4$ shell on the UCNP core and demonstrates why the XRD pattern of the core/shell type UCNP is very similar to that of the core UCNP. The *d*-spacing from HRTEM was determined to be 0.268 nm, which matches well with the distance between

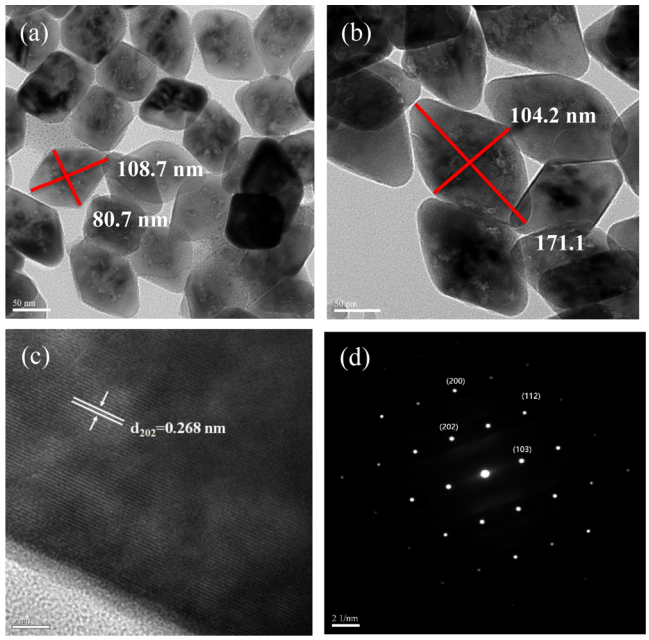

Figure 4. HRTEM images (×500 K) of (a) $LiYF_4:Yb^{3+}_{0.25},Tm^{3+}_{0.01}$ core UCNP and (b) $LiYF_4:Yb^{3+}_{0.25},Tm^{3+}_{0.01}@LiYF_4:Yb^{3+}_{0.2}$ core/shell UCNP. (c) HRTEM image (×300 K) of the single-crystalline structure of the $LiYF_4:Yb^{3+}_{0.25},Tm^{3+}_{0.01}@LiYF_4:Yb^{3+}_{0.2}$ core/shell UCNP. (d) SAED pattern of the $LiYF_4:Yb^{3+}_{0.25},Tm^{3+}_{0.01}@LiYF_4:Yb^{3+}_{0.2}$ core/shell UCNP.

the (202) planes in $LiYF_4$ (Figure 4c). The selected area electron diffraction (SAED) pattern in Figure 4d shows that

DOI: 10.1021/acsomega.8b03414
ACS Omega 2019, 4, 3322−3328

the SAED pattern consists of many spots, which demonstrates that the $LiYF_4$ core/shell UCNP has the single-crystal structure. The SAED pattern further illustrates the formation of the tetragonal phase of the core/shell UCNP and is indexed to the corresponding (*hkl*) planes according to the standard JCPDS no. 17-0874.

Because our research goal was to prepare a kind of UCNP with the function of emitting UV radiation to disrupt the micelles of the dual-stimuli BCP, the intensity of UV emission in relation to the doping concentrations of Yb^{3+} sensitizer and Tm^{3+} activator was studied. It was found that an optimum combination of Yb^{3+} and Tm^{3+} was 25 mol % Yb^{3+} and 1 mol % Tm^{3+} for the UCNP core. As for the shell of the UCNP, only Yb^{3+} sensitizer was needed to be used as the dopant of the $LiYF_4$ host material, and the optimal ratio was around 20 mol %.

The PL spectra of the colloidal $LiYF_4:Yb^{3+},Tm^{3+}$ UCNP core and $LiYF_4:Yb^{3+},Tm^{3+}@LiYF_4:Yb^{3+}$ core/shell UCNP under laser excitation at 980 nm are shown in Figure 5.

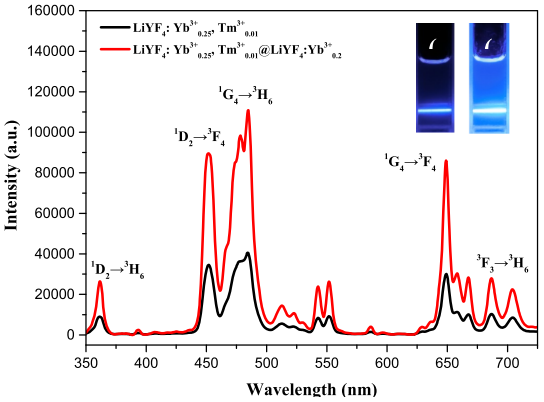

Figure 5. PL spectra of the $LiYF_4:Yb^{3+}_{0.25},Tm^{3+}_{0.01}$ core UCNP and $LiYF_4:Yb^{3+}_{0.25},Tm^{3+}_{0.01}@LiYF_4:Yb^{3+}_{0.2}$ core/shell UCNP under 980 nm NIR irradiation. The insets (from left to right) are the corresponding luminescence photographs of solutions of the core UCNP and core/shell UCNP, respectively.

Several PL bands ranging from the UV to visible region are observed. For both core UCNP and core/shell UCNP, it can be found that their maxima are at 362, 451, 484, 649, and 687 nm, which correspond to $^1D_2 \rightarrow {}^3H_6$, $^1D_2 \rightarrow {}^3F_4$, $^1G_4 \rightarrow {}^3H_6$, $^1G_4 \rightarrow {}^3F_4$, and $^3F_3 \rightarrow {}^3H_6$, respectively. The UV range before 350 nm is beyond the detection range of our spectrometer setup. It is striking that the intensities of all PL bands are much enhanced after overcoating the shell. This is very beneficial for the disruption of the BCP which contains photoresponsive segment units.

In the preparation of the BCP for controlled release of drugs via the dual-stimuli function, we have synthesized an amphiphilic dual-stimuli BCP composed of a thermoresponsive building block and a photoresponsive building block. The thermoresponsive block was synthesized from *N*,*N*-diethylacrylamide (DEAAm) and functions as the hydrophilic segment, while the photoresponsive block was synthesized from 2-nitrobenzyl acrylate (NBA) and functions as the hydrophobic segment. The as-synthesized dual-stimuli BCP was characterized by proton nuclear magnetic resonance (^{1}H NMR), IR, gel permeation chromatography (GPC), and differential scanning calorimetry (DSC) (Supporting Information). The number average molecular weight ($\overline{M}_n$) of the copolymer PDEAAm-*b*-PNBA is shown in Figure S3 (Supporting Information). It is ca. 11 000 g/mol with a polydispersity index of 1.28. Because the ratio of *m* and *n* of the copolymer PDEAAm-*b*-PNBA obtained from the ^{1}H NMR spectrum (Figure S1, Supporting Information) is about 1:3, the average values of *m* and *n* calculated are ca. 18.3 and 54.8, respectively.

NR is a common dye and was used as a model drug to simulate the process of controlled release of drugs. After UCNP and NR were encapsulated into the amphiphilic BCP, the NR-loaded UCNP@BCP hybrid was first dissolved in tetrahydrofuran (THF). Subsequently, the solution was poured into water and then THF was evaporated to form an amphiphilic micelle solution in aqueous media. The HRTEM images of the UCNP-loaded BCP micelles and the UCNP and NR co-loaded BCP micelles are shown in Figures S5 and S6 (Supporting Information). From both figures, it is apparent that UCNPs are loaded into the BCP micelles. Upon NIR irradiation at 980 nm, the nitrobenzyl groups on the PNBA block were cleaved because of the 362 nm UV radiation emitted by UCNPs. Photocleavage of the nitrobenzyl groups converted the PNBA block into the hydrophilic polyacrylic acid, which rendered the disruption of the micelles and the release of NR. On the other hand, after raising the temperature above the LCST of the amphiphilic BCP, the micelles contracted and the NR molecules in the micelles were squeezed out. Hence, the controlled release of drugs could be proceeded by two different ways via the dual-stimuli BCP.

To illustrate the trigger function of drug release by using the micelle solution formed from the UCNP-loaded BCP, we further performed experiments to ensure the dissociation of micelles upon exposure of NR-loaded UCNP@BCP nanocarriers under irradiation of a 980 nm NIR laser diode. For comparison, the NR-loaded UCNP@BCP micellar solution was irradiated with UV and NIR light. Because NR is a hydrophobic dye and emits light around 625 nm, the emission intensity of the NR-loaded UCNP@BCP micellar solution in water under 365 nm UV or 980 nm NIR light irradiation was measured. As shown in Figure 6a, the PL intensity of NR decreases with the increase of irradiation time of UV light, indicating that more NR dye was released to water from the micelles. Because the NR dye was hydrophobic, if more NR dye remained in micelles, the PL intensity around 625 nm would be stronger. Hence, the decrease of PL intensity indicates that more of the *o*-nitrobenzyl moieties in the micelle core were cleaved by UV light and the PNBA block turned into the hydrophilic polyacrylic acid segment. To demonstrate the trigger function by the as-synthesized UCNP, the NR-loaded UCNP@BCP micellar solution was irradiated under NIR light; it was also found that the PL intensity of NR decreases with the increase of irradiation time (Figure 6b). Although the irradiation time is much longer than that of the micellar solution irradiated directly by UV light, this may be a beneficial factor for use in the drug delivery of an extended-release formulation. Moreover, as mentioned above, NIR irradiation is less detrimental and has deeper penetration to organisms compared to UV/vis light. The PL results strongly support that the core/shell UCNPs were encapsulated by the BCP and could emit UV light under NIR irradiation. The photos in the insets of Figure 6a,b display that after longer irradiation time, the purple color would turn into a light color because more NR molecules were released into water. This is a strong evidence to illustrate that our UCNP@BCP hybrid can be used to control the drug release.

DOI: 10.1021/acsomega.8b03414
ACS Omega 2019, 4, 3322−3328

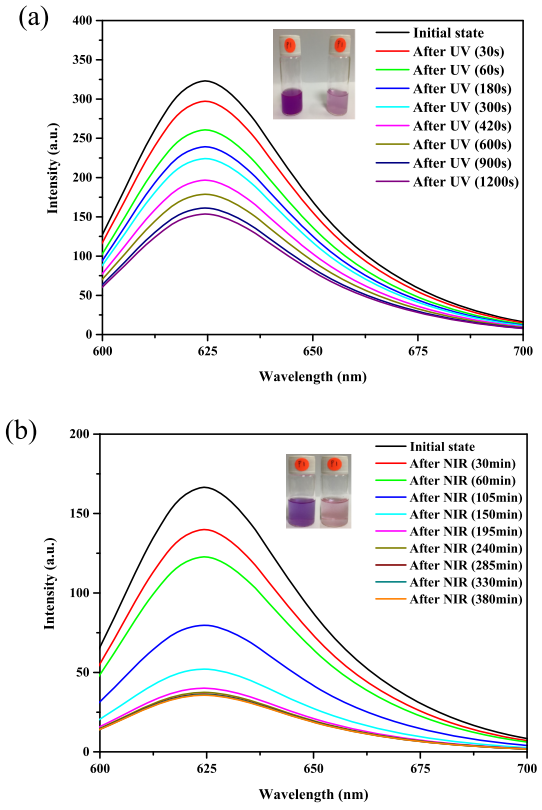

Figure 6. Emission spectra of NR ($\lambda_{excitation}$ = 550 nm) for the micellar solution with both UCNPs and NR loaded under (a) 365 nm UV irradiation or (b) 980 nm NIR light exposure. The insets (from left to right) are the corresponding photographs of the micellar solutions before and after UV or NIR irradiation.

Furthermore, to test the function of the thermoresponsive block of the BCP, we carried out an experiment to detect the LCST of PDEAAm-*b*-PNBA. It was found that the polymeric solution turned turbid when the temperature was raised above 25 °C (Figure 7a). It indicated that the amphiphilic BCP turned hydrophobic in aqueous media because of the PDEAAm thermoresponsive segment and the LCST of PDEAAm-*b*-PNBA was around 25 °C. Subsequently, we studied the controlled-release process of the loaded NR molecules triggered by the thermoresponsive block. As shown in Figure 7b, it can be found that the emission intensity around 625 nm decreases with the increase of the temperature. We tested the temperature from 20 to 37 °C to simulate the drug release process in the human body. The result indicates that the NR dye has been squeezed out from the NR-loaded micelles because of the contraction of the polymeric micelles above the LCST of PDEAAm-*b*-PNBA.

3. CONCLUSIONS

In summary, an amphiphilic photoresponsive and thermoresponsive BCP which contains both thermoresponsive *N*-alkyl-substituted acrylamide group and photoresponsive *o*-nitrobenzyl group has been successfully synthesized. To achieve the design goal of using this dual-stimuli BCP in controlled release of drugs under photostimulation conditions, a core/shell UCNP with the structure of $LiYF_4:Yb^{3+}_{0.25},Tm^{3+}_{0.01}$@$LiYF_4:Yb^{3+}_{0.2}$ and anti-Stokes emission of UV light was prepared and loaded into the polymeric micelles. Upon NIR light exposure, the BCP displayed an extended release of the model drug NR because of the disruption of the BCP in the aqueous solution. Alternatively, in the case of the BCP in which only NR was loaded, the behavior of the controlled release could be observed when the temperature was raised above the LCST of the BCP. Both results confirmed that the synthesized PDEAAm-*b*-PNBA BCP in conjunction with the $LiYF_4$ core/shell UCNP could be applied as an effective nanocarrier for controlled release of drugs under the stimulation of photochange or temperature change.

4. EXPERIMENTAL SECTION

4.1. Synthesis of the Core UCNP $LiYF_4:Yb^{3+}_{0.25},Tm^{3+}_{0.01}$. UCNPs of $LiYF_4$ doped with 25% of Yb^{3+} and 1% Tm^{3+} ions were synthesized by the thermal decomposition approach. At first, thulium and lithium trifluoroacetate precursors in the presence of oleic acid coordinating ligands and non-coordinating 1-octadecene solvent molecules were prepared. First, 0.1094 g (1.48 mmol) of Li_2CO_3, 0.1671 g of Y_2O_3 (0.74 mmol), 0.0985 g (0.25 mmol) of Yb_2O_3, and 0.0039 g (0.01 mmol) of Tm_2O_3 were dissolved in 10 mL of 50% (v/v % in water) concentrated trifluoroacetic acid in a three-necked 100 mL flask and heated at 90 °C for 30 min. Next, 15 mL of oleic acid and 15 mL of 1-octadecene were added into the three-necked flask. The resulting solution was then heated at 120 °C under vacuum for 30 min with magnetic stirring to remove water and oxygen.

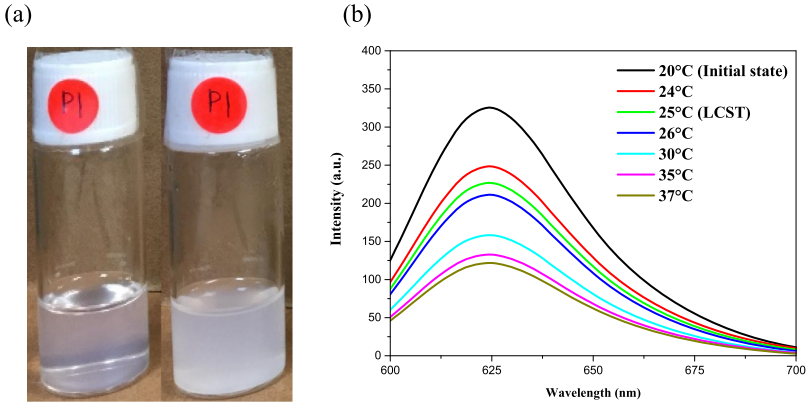

Figure 7. (a) Photographs show the BCP aqueous solutions below (left) and above (right) the LCST of PDEAAm-*b*-PNBA. (b) Emission spectra of NR ($\lambda_{excitation}$ = 550 nm) for the micellar solution with only NR loaded under the temperature change.

DOI: 10.1021/acsomega.8b03414
ACS Omega 2019, 4, 3322−3328

The light yellow solution was then heated to 300 °C at a rate of about 30 °C per minute under argon gas protection and kept at this temperature under vigorous stirring for about 1 h. The reaction mixture was cooled to room temperature and precipitated in ethanol and collected by centrifugation at 8000 rpm for 10 min. The precipitate was dissolved in hexane and then reprecipitated in ethanol. The procedure was repeated two times, and the nanoparticles were dispersed in 10 mL of hexane for further synthesis steps.

4.2. Synthesis of the Core/Shell UCNP $LiYF_4:Yb^{3+}_{0.25},Tm^{3+}_{0.01}@LiYF_4:Yb^{3+}_{0.2}$. The procedure for the growth of the shell on the core UCNP is similar to that of the synthesis of the core UCNP. First, 0.1182 g (1.60 mmol) of Li_2CO_3, 0.1806 g of Y_2O_3 (0.80 mmol), and 0.0788 g (0.20 mmol) of Yb_2O_3 were dissolved in 10 mL of 50% (v/v % in water) concentrated trifluoroacetic acid in a three-necked 100 mL flask and heated at 90 °C for 30 min. Next, 15 mL of oleic acid and 15 mL of 1-octadecene were added into the three-necked flask. The resulting solution was then heated at 120 °C under vacuum for 30 min. At this time, the core solution was poured into the flask. The reaction was continued until the solution turned light yellow to remove hexane and water. The reaction mixture was then heated to 300 °C at a rate of about 30 °C per minute under argon gas protection and kept at this temperature under vigorous stirring for about 1 h. The reaction mixture was cooled to room temperature, and the product was precipitated and purified according to the procedures as mentioned above. Thus, the active-core/active-shell structured UCNPs were obtained.

4.3. Synthesis of the BCP PDEAAm-*b*-PNBA. NBA was prepared according to the reported procedure.[34] The amphiphilic BCP of PDEAAm-*b*-PNBA was synthesized by ATRP. At first, DEAAm (2.3 g, 18 mmol) was dissolved in 8 mL dimethyl sulfoxide (DMSO). The solution was degassed three times using the freeze−pump−thaw procedure under the protection of an argon atmosphere. Next, the purified CuBr (0.015 g, 0.11 mmol) and bipyridine (0.02 g, 0.13 mmol) were added sequentially. After the initiator, 1-bromoethyl benzene (0.12 g, 0.6 mmol), was added, the reaction mixture was heated at 80 °C for 3 h. The synthesized PDEAAm was used as a macroinitiator agent to polymerize with NBA. The NBA (0.38 g, 1.8 mmol) in 1 mL DMSO was also degassed three times using the freeze−pump−thaw procedure and sealed under vacuum. Thereafter, the NBA monomer was added into the flask and the reaction was continued for 3 h at 80 °C. Then, the mixture was exposed to air and cooled to room temperature to quench the polymerization. Afterward, the flask was removed from the oil bath and the reaction mixture was diluted with THF. The solution was filtered through a column with neutral alumina to remove the catalyst. The final BCP was recovered by precipitation in methanol, filtering, and then drying under vacuum for 48 h.

4.4. Characterization. The XRD patterns of the core UCNP and core/shell UCNP were obtained by using a Bruker D8 ADVANCE diffractometer, using Cu Kα radiation with a step size of 0.05° and a scanning speed of 4°/min. TEM images were obtained with a JEOL JEM-1230 transmission electron microscope. UV/vis spectra were collected on a PerkinElmer Lambda 35 UV−vis spectrophotometer. PL spectra were recorded on a Hitachi F-7000 fluorescence spectrophotometer. Upconversion PL measurements were performed on a Ray Lead Tech. spectrofluorometer. A 980 nm laser diode (SDL-980-LM-5000T-Diode Laser) with a power of 3 W/cm^2 was employed as the excitation source. Infrared spectra of the samples were obtained with a Bio-Rad FTS 165 Fourier transform infrared spectrometer over the frequency range of 4000−400 cm^{-1} at a resolution of 4 cm^{-1}. ^{1}H NMR spectra were recorded on a Bruker AVANCE 400 FT-NMR spectrometer with tetramethylsilane as the internal standard. The molecular weight of the BCP was determined by GPC using a Young Lin Acme 9000 liquid chromatograph equipped with a 410 refractive index detector and μ-Styragel columns with THF as the carrier solvent and polystyrene standards used for calibration.

■ ASSOCIATED CONTENT

Supporting Information

The Supporting Information is available free of charge on the ACS Publications website at DOI: 10.1021/acsomega.8b03414.

^{1}H NMR spectrum, IR spectrum, GPC curve and data, and DSC thermogram of PDEAAm-*b*-PNBA and HRTEM images of UCNP-loaded BCP micelles and UCNP and NR co-loaded BCP micelles (PDF)

■ AUTHOR INFORMATION

Corresponding Author

*E-mail: tlwang@nuk.edu.tw. Phone: (+886)-7-5919278. Fax: (+886)-7-5919277.

ORCID

Chien-Hsin Yang: 0000-0001-8772-9715

Tzong-Liu Wang: 0000-0002-9144-850X

Notes

The authors declare no competing financial interest.

■ ACKNOWLEDGMENTS

We gratefully acknowledge the support of the Ministry of Science and Technology in Taiwan through Grant MOST 105-2221-E-390-029.

■ REFERENCES

(1) Masci, G.; Giacomelli, L.; Crescenzi, V. Atom Transfer Radical Polymerization ofN-Isopropylacrylamide. *Macromol. Rapid Commun.* **2004**, *25*, 559−564.

(2) Sugihara, S.; Kanaoka, S.; Aoshima, S. Double thermosensitive diblock copoly-mers of vinyl ethers with pendant oxyethylene groups: Unique physical gelation. *Macromolecules* **2005**, *38*, 1919−1927.

(3) Liu, S.; Armes, S. P. Synthesis and aqueous solution behavior of a pH-responsive schizophrenic diblock copolymer. *Langmuir* **2003**, *19*, 4432−4438.

(4) Yusa, S.-i.; Shimada, Y.; Mitsukami, Y.; Yamamoto, T.; Morishima, Y. pH-Responsive Micellization of Amphiphilic Diblock Copolymers Synthesized via Reversible Addition−Fragmentation Chain Transfer Polymerization. *Macromolecules* **2003**, *36*, 4208−4215.

(5) Shimoboji, T.; Ding, Z. L.; Stayton, P. S.; Hoffman, A. S. Photoswitching of Ligand Association with a Photoresponsive Polymer−Protein Conjugate. *Bioconjugate Chem.* **2002**, *13*, 915−919.

(6) Zhu, Z.; Xu, J.; Zhou, Y.; Jiang, X.; Armes, S. P.; Liu, S. Effect of salt on the micellization kinetics of pH-responsive abc triblock copolymers. *Macromolecules* **2007**, *40*, 6393−6400.

(7) Schattling, P.; Jochum, F. D.; Theato, P. Multi-stimuli responsive polymers - the all-in-one talents. *Polym. Chem.* **2014**, *5*, 25−36.

(8) Zhuk, A.; Mirza, R.; Sukhishvili, S. Multiresponsive clay-containing layer-by-layer films. *ACS Nano* **2011**, *5*, 8790−8799.

DOI: 10.1021/acsomega.8b03414
ACS Omega 2019, 4, 3322−3328

(9) He, Z.; Satarkar, N.; Xie, T.; Cheng, Y.-T.; Hilt, J. Z. Remote controlled multishape polymer nanocomposites with selective radio-frequency actuations. *Adv. Mater.* **2011**, *23*, 3192−3196.
(10) Jordão, N.; Gavara, R.; Parola, A. J. Flavylium-supported poly(*N*-isopropylacrylamide): a class of multistimuli responsive polymer. *Macromolecules* **2013**, *46*, 9055−9063.
(11) Yang, F.; Cao, Z.; Wang, G. Micellar assembly of a photo- and temperature-responsive amphiphilic block copolymer for controlled release. *Polym. Chem.* **2015**, *6*, 7995−8002.
(12) Liras, M.; González-Béjar, M.; Peinado, E.; Francés-Soriano, L.; Pérez-Prieto, J.; Quijada-Garrido, I.; García, O. Thin amphiphilic polymer-capped upconversion nanoparticles: enhanced emission and thermoresponsive properties. *Chem. Mater.* **2014**, *26*, 4014−4022.
(13) Wang, F.; Liu, X. Recent advances in the chemistry of lanthanide-doped upconversion nanocrystals. *Chem. Soc. Rev.* **2009**, *38*, 976−989.
(14) Chen, Z.; Chen, H.; Hu, H.; Yu, M.; Li, F.; Zhang, Q.; Zhou, Z.; Yi, T.; Huang, C. Versatile Synthesis Strategy for Carboxylic Acid−functionalized Upconverting Nanophosphors as Biological Labels. *J. Am. Chem. Soc.* **2008**, *130*, 3023−3029.
(15) Carling, C.-J.; Nourmohammadian, F.; Boyer, J.-C.; Branda, N. R. Remote-Control Photorelease of Caged Compounds Using Near-Infrared Light and Upconverting Nanoparticles. *Angew. Chem., Int. Ed.* **2010**, *49*, 3782−3785.
(16) Yan, B.; Boyer, J.-C.; Branda, N. R.; Zhao, Y. Near-infrared light-triggered dissociation of block copolymer micelles using upconverting nanoparticles. *J. Am. Chem. Soc.* **2011**, *133*, 19714−19717.
(17) Xiang, J.; Tong, X.; Shi, F.; Yan, Q.; Yu, B.; Zhao, Y. Near-infrared light-triggered drug release from UV-responsive diblock copolymer-coated upconversion nanoparticles with high monodispersity. *J. Mater. Chem. B* **2018**, *6*, 3531−3540.
(18) Zhao, T.; Wang, P.; Li, Q.; Al-Khalaf, A. A.; Hozzein, W. N.; Zhang, F.; Li, X.; Zhao, D. Near-infrared triggered decomposition of nanocapsules with high tumor accumulation and stimuli responsive fast elimination. *Angew. Chem., Int. Ed.* **2018**, *57*, 2611−2615.
(19) Chen, G.; Jaskula-Sztul, R.; Esquibel, C. R.; Lou, I.; Zheng, Q.; Dammalapati, A.; Harrison, A.; Eliceiri, K. W.; Tang, W.; Chen, H.; Gong, S. Neuroendocrine Tumor-Targeted Upconversion Nanoparticle-Based Micelles for Simultaneous NIR-Controlled Combination Chemotherapy and Photodynamic Therapy, and Fluorescence Imaging. *Adv. Funct. Mater.* **2017**, *27*, 1604671.
(20) Wang, F.; Banerjee, D.; Liu, Y.; Chen, X.; Liu, X. Upconversion nanoparticles in biological labeling, imaging, and therapy. *Analyst* **2010**, *135*, 1839−1854.
(21) Gnach, A.; Bednarkiewicz, A. Lanthanide-doped up-converting nanoparticles: merits and challenges. *Nano Today* **2012**, *7*, 532−563.
(22) Carling, C.-J.; Boyer, J.-C.; Branda, N. R. Remote-control photoswitching using NIR Light. *J. Am. Chem. Soc.* **2009**, *131*, 10838−10839.
(23) Boyer, J.-C.; Carling, C.-J.; Gates, B. D.; Branda, N. R. Two-way photoswitching using one type of near-infrared light, upconverting nanoparticles, and changing only the light intensity. *J. Am. Chem. Soc.* **2010**, *132*, 15766−15772.
(24) Qian, H.-S.; Zhang, Y. Synthesis of Hexagonal-Phase Core−Shell NaYF4Nanocrystals with Tunable Upconversion Fluorescence. *Langmuir* **2008**, *24*, 12123−12125.
(25) Chen, G.; Qiu, H.; Prasad, P. N.; Chen, X. Upconversion nanoparticles: design, nanochemistry, and applications in theranostics. *Chem. Rev.* **2014**, *114*, 5161−5214.
(26) Yang, D.; Ma, P. a.; Hou, Z.; Cheng, Z.; Li, C.; Lin, J. Current advances in lanthanide ion (Ln3+)-based upconversion nanomaterials for drug delivery. *Chem. Soc. Rev.* **2015**, *44*, 1416−1448.
(27) Huang, X.; Lin, J. Active-core/active-shell nanostructured design: an effective strategy to enhance Nd3+/Yb3+ cascade sensitized upconversion luminescence in lanthanide-doped nanoparticles. *J. Mater. Chem. C* **2015**, *3*, 7652−7657.
(28) Wang, X.; Xu, T.; Bu, Y.; Yan, X. Giant enhancement of upconversion emission in NaYF4:Er3+@NaYF4:Yb3+ active-core/active-shell nanoparticles. *RSC Adv.* **2016**, *6*, 22845−22851.
(29) Du, X.; Wang, X.; Meng, L.; Bu, Y.; Yan, X. Enhance the Er^{3+} Upconversion Luminescence by Constructing $NaGdF_4$:Er^{3+}@$NaGdF_4$:Er^{3+} Active-Core/Active-Shell Nanocrystals. *Nanoscale Res. Lett.* **2017**, *12*, 163.
(30) Klán, P.; Šolomek, T.; Bochet, C. G.; Blanc, A.; Givens, R.; Rubina, M.; Popik, V.; Kostikov, A.; Wirz, J. Photoremovable protecting groups in chemistry and biology: reaction mechanisms and efficacy. *Chem. Rev.* **2012**, *113*, 119−191.
(31) Pelliccioli, A. P.; Wirz, J. Photoremovable protecting groups: reaction mechanisms and applications. *Photochem. Photobiol. Sci.* **2002**, *1*, 441−458.
(32) Furuta, F. Coumarin-4-ylmethyl Phototriggers. In *Dynamic Studies in Biology: Phototriggers, Photoswitches and Caged Biomolecules*; Goeldner, M., Givens, R., Eds.; Wiley-VCH: Weinheim, 2005; pp 29−55.
(33) Roy, D.; Brooks, W. L. A.; Sumerlin, B. S. New directions in thermoresponsive polymers. *Chem. Soc. Rev.* **2013**, *42*, 7214−7243.
(34) Jiang, X.; Lavender, C. A.; Woodcock, J. W.; Zhao, B. Multiple Micellization and Dissociation Transitions of Thermo- and Light-Sensitive Poly(ethylene oxide)-*b*-poly(ethoxytri(ethylene glycol) acrylate-*co*-*o*-nitrobenzyl acrylate) in Water. *Macromolecules* **2008**, *41*, 2632−2643.

DOI: 10.1021/acsomega.8b03414
ACS Omega 2019, 4, 3322−3328